

# A Mononuclear Non-Heme High-Spin Iron(III)–Hydroperoxo Complex as an Active Oxidant in Sulfoxidation Reactions

Yun Mi Kim,<sup>†,||</sup> Kyung-Bin Cho,<sup>†,||</sup> Jaeheung Cho,<sup>†,§</sup> Binju Wang,<sup>‡</sup> Chunsen Li,<sup>‡</sup> Sason Shaik,<sup>\*,‡</sup> and Wonwoo Nam<sup>\*,†</sup>

<sup>†</sup>Department of Bioinspired Science, Ewha Womans University, Seoul 120-750, Korea

<sup>‡</sup>Institute of Chemistry and the Lise Meitner–Minerva Center for Computational Quantum Chemistry, The Hebrew University of Jerusalem, 91904 Jerusalem, Israel

<sup>§</sup>Department of Emerging Materials Science, DGIST, Daegu 711-873, Korea

## S Supporting Information

**ABSTRACT:** We report the first direct experimental evidence showing that a high-spin iron(III)–hydroperoxo complex bearing an N-methylated cyclam ligand can oxidize thioanisoles. DFT calculations showed that the reaction pathway involves heterolytic O–O bond cleavage and that the choice of the heterolytic pathway versus the homolytic pathway is dependent on the spin state and the number of electrons in the  $d_{xz}$  orbital of the  $\text{Fe}^{\text{III}}\text{–OOH}$  species.

Elucidation of the nature of reactive intermediates in the catalytic cycles of dioxygen activation and oxygenation reactions by heme and non-heme iron enzymes has been the subject of intense research in bioinorganic and biological chemistry. High-valent iron–oxo species, such as  $\text{Fe}^{\text{IV}}\text{O}$  porphyrin  $\pi$ -cation radicals in cytochrome P450 (P450) and non-heme  $\text{Fe}^{\text{IV}}\text{O}$  intermediates, have been invoked as active oxidants that effect the oxygenation of organic substrates.<sup>1,2</sup> In biomimetic studies, it has been demonstrated that  $\text{Fe}^{\text{IV}}\text{O}$  complexes are strong oxidants that can oxygenate various organic substrates, such as in hydroxylation and sulfoxidation reactions.<sup>3</sup>

In addition to  $\text{Fe}^{\text{IV}}\text{O}$  intermediates, iron(III)–hydroperoxo ( $\text{Fe}^{\text{III}}\text{–OOH}$ ) species have been proposed as a “second electrophilic oxidant” in oxygenation reactions,<sup>4,5</sup> particularly in the sulfoxidation of thioether substrates by P450 and its analogues.<sup>6</sup>  $\text{Fe}^{\text{III}}\text{–OOH}$  species have also been proposed as active oxidants in non-heme iron systems, including bleomycin, Rieske dioxygenases, and synthetic iron catalysts.<sup>7</sup> However, experimental evidence against the  $\text{Fe}^{\text{III}}\text{–OOH}$  species as a “second electrophilic oxidant” recently appeared in iron model reactions.<sup>8</sup> In addition, computational studies by one of us<sup>9</sup> have shown that  $\text{Fe}^{\text{III}}\text{–OOH}$  species are sluggish oxidants in oxygenation reactions, including in sulfoxidation by the  $\text{Fe}^{\text{III}}\text{–OOH}$  porphyrin species known as Compound 0 (Cpd 0) in P450. Thus, there has been an intriguing, continuing controversy over the involvement of  $\text{Fe}^{\text{III}}\text{–OOH}$  species as a “second electrophilic oxidant” in the reactions of heme and non-heme iron enzymes and their model compounds.<sup>4–9</sup>

Recently, a high-spin (HS)  $\text{Fe}^{\text{III}}\text{–OOH}$  complex bearing a macrocyclic N-methylated cyclam as a supporting ligand,

$[(\text{TMC})\text{Fe}^{\text{III}}(\text{OOH})]^{2+}$  (**1**) (TMC = 1,4,8,11-tetramethyl-1,4,8,11-tetraazacyclotetradecane), was synthesized and characterized with various spectroscopic methods.<sup>10</sup> Interestingly, this HS  $\text{Fe}^{\text{III}}\text{–OOH}$  complex showed reactivities in nucleophilic and electrophilic reactions,<sup>10a</sup> providing direct experimental evidence for the involvement of HS  $\text{Fe}^{\text{III}}\text{–OOH}$  complexes in the oxidation of organic substrates. More recently, the reactivities of HS and low-spin (LS) non-heme  $\text{Fe}^{\text{III}}\text{–OOH}$  complexes in H-atom abstraction (HAA) reactions were investigated experimentally and theoretically, and HS  $\text{Fe}^{\text{III}}\text{–OOH}$  was found to be an active oxidant in HAA.<sup>11</sup>

As mentioned above, the involvement of Cpd 0 in sulfoxidation by P450 and its analogues has been debated over two decades.<sup>6</sup> Similarly, no direct experimental evidence for the involvement of  $\text{Fe}^{\text{III}}\text{–OOH}$  species as active oxidants in oxygen-atom transfer (OAT) reactions has been obtained using non-heme iron models. We now report that the HS  $\text{Fe}^{\text{III}}\text{–OOH}$  complex **1** is a competent oxidant in the oxidation of sulfides to give the corresponding sulfoxides. In contrast, a LS  $\text{Fe}^{\text{III}}\text{–OOH}$  complex was found to be a sluggish oxidant in sulfoxidations. The mechanisms of sulfoxidation by **1** in addition to LS  $\text{Fe}^{\text{III}}\text{–OOH}$  complexes were investigated by density functional theory (DFT),<sup>12</sup> leading to a proposed heterolytic O–O bond-breaking transition state (TS) in the OAT reaction by **1** (Figure 1).

*Experimental studies.* Complex **1**, which was prepared by adding 10 equiv of  $\text{HClO}_4$  to a solution of  $[(\text{TMC})\text{Fe}^{\text{III}}(\text{O}_2)]^+$  in 3:1 acetone/ $\text{CF}_3\text{CH}_2\text{OH}$  at  $-20^\circ\text{C}$ , decayed with a rate

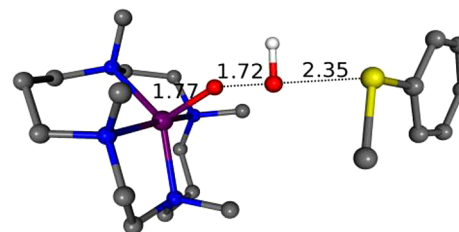


**Figure 1.** DFT-optimized transition state for the sulfoxidation of thioanisole by **1**. H atoms except for O–H have been omitted for clarity. Atom colors: Fe, purple; N, blue; O, red; S, yellow; C, grey; H, white. The Fe–O, O–O, and O–S distances (in Å) are shown.

Received: April 26, 2013

Published: May 30, 2013

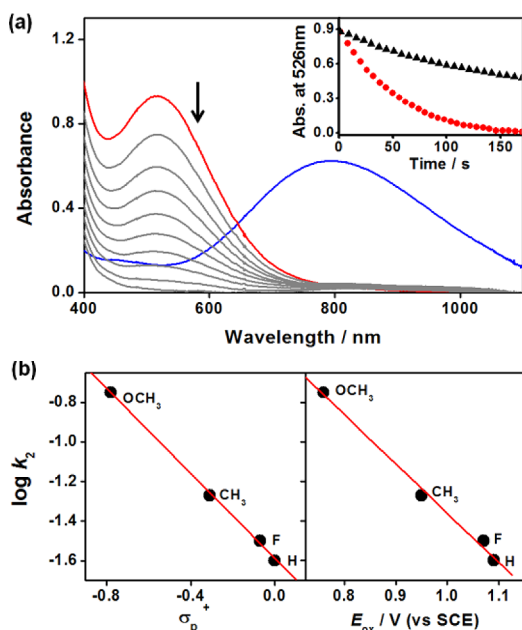


**Figure 2.** (a) UV-vis spectral changes showing the conversion of  $[(\text{TMC})\text{Fe}^{\text{III}}(\text{O}_2)]^+$  (1 mM, blue line) to  $[(\text{TMC})\text{Fe}(\text{OOH})]^{2+}$  (**1**) (red line) upon the addition of 10 equiv of  $\text{HClO}_4$  and the reaction of **1** with 4-methoxythioanisole (4-MTA) (100 mM) in 3:1 acetone/ $\text{CF}_3\text{CH}_2\text{OH}$  at  $-20^\circ\text{C}$ . The inset shows the time courses of the absorbance changes for **1** at 526 nm for the natural decay (black  $\blacktriangle$ ) and the reaction with 4-MTA (red  $\bullet$ ). (b) Plots of (left)  $\log k_2$  vs  $\sigma_p^+$  (Hammett plot) and (right)  $\log k_2$  vs  $E_{\text{ox}}$  for  $p\text{-X-C}_6\text{H}_4\text{SCH}_3$ .

constant  $k_{\text{obs}} = 3.3 \times 10^{-3} \text{ s}^{-1}$  (Figure 2a inset), forming  $[(\text{TMC})\text{Fe}^{\text{IV}}(\text{O})]^{2+}$  (**2**) [Figure S1 in the Supporting Information (SI)].<sup>10a</sup> Interestingly, upon the addition of 4-methoxythioanisole (4-MTA) to the solution of **1**, this intermediate disappeared at a higher rate ( $k_{\text{obs}} = 2.1 \times 10^{-2} \text{ s}^{-1}$  at  $-20^\circ\text{C}$ ) under pseudo-first-order conditions (Figure 2a). The rate constant increased linearly with increasing substrate concentration (Figure S2 and Table S1). The reaction rate was temperature-dependent; the Eyring plot between 233 and 263 K was linear and gave the activation parameters  $\Delta H^\ddagger = 39 \text{ kJ mol}^{-1}$  and  $\Delta S^\ddagger = -119 \text{ J mol}^{-1} \text{ K}^{-1}$  (Figure S3). When **1** was reacted with *para*-substituted thioanisoles ( $p\text{-X-C}_6\text{H}_4\text{SCH}_3$ , X =  $\text{OCH}_3$ ,  $\text{CH}_3$ , F, H) to investigate the electronic effect of the substrate on the sulfoxidation reaction, a  $\rho$  value of  $-1.1$  was obtained from the Hammett plot of the second-order rate constant ( $k_2$ ) versus  $\sigma_p^+$  (Figure 2b, left panel; also see Figure S4 and Table S1). This result indicates the electrophilic character of the hydroperoxo group of **1** in the sulfoxidation of sulfides, as frequently observed in sulfoxidation reactions by high-valent metal-oxo complexes.<sup>13</sup> In addition, we observed a good linear correlation with a slope of  $-2.5$  when the rate constant was plotted versus the oxidation potential ( $E_{\text{ox}}$ ) of  $p\text{-X-C}_6\text{H}_4\text{SCH}_3$  (Figure 2b, right panel; also see Table S1), suggesting that the oxidation of sulfides by **1** occurs via a direct OAT mechanism.<sup>13</sup>

Product analysis of the reaction solution revealed that methyl phenyl sulfoxide was formed as the sole product in high yield ( $\sim 80\%$  based on the amount of **1** used), and the source of oxygen in the sulfoxide product was found to be the hydroperoxo ligand of **1** when the reaction was performed with  $^{18}\text{O}$ -labeled **1** (i.e.,  $[(\text{TMC})\text{Fe}^{\text{III}}(^{18}\text{O}^{18}\text{OH})]^{2+}$ ) (Figure S5). In addition, by analyzing the reaction solution with electron paramagnetic resonance (EPR) spectroscopy and electrospray ionization mass

spectrometry (ESI-MS), we found that an  $\text{Fe}^{\text{II}}$  species was formed as a major decomposed product of the  $\text{Fe}^{\text{III}}\text{OH}$  complex resulting from the sulfoxidation reaction (Figures S6 and S7).<sup>14</sup>

For comparison, the reactivity of the LS  $\text{Fe}^{\text{III}}\text{-OOH}$  complex  $[(\text{N4Py})\text{Fe}^{\text{III}}(\text{OOH})]^{2+}$  (**3**) [ $\text{N4Py} = N,N\text{-bis}(2\text{-pyridylmethyl})\text{-}N\text{-(bis}(2\text{-pyridyl)methyl)amine}]^{15}$  was investigated in the sulfoxidation reaction. Addition of 4-MTA to a reaction solution of **3** in  $\text{CH}_3\text{OH}$  at  $25^\circ\text{C}$  did not have much effect on the rate of disappearance of **3** (Figure S8),<sup>16</sup> suggesting that the LS  $\text{Fe}^{\text{III}}\text{-OOH}$  complex is a sluggish oxidant for the oxidation of thioanisoles.

The reactivity of **1** was also compared with that of the corresponding  $\text{Fe}^{\text{IV}}\text{O}$  complex **2**. Interestingly, **1** ( $k_2 = 1.8 \times 10^{-1} \text{ M}^{-1} \text{ s}^{-1}$ ) was more reactive than **2** ( $k_2 = 1.7 \times 10^{-2} \text{ M}^{-1} \text{ s}^{-1}$ ) by a factor of 10 in the oxidation of 4-MTA (Figure S9). However, when the proton effect on the reactivity of non-heme  $\text{Fe}^{\text{IV}}\text{O}$  complexes was considered,<sup>17</sup> **2** was more reactive than **1** in the presence of  $\text{HClO}_4$  (10 equiv relative to **2**) (Figure S10). It is worth noting that in contrast to  $\text{Fe}^{\text{IV}}\text{O}$  complexes, there was no significant proton effect on the reactivity of the  $\text{Fe}^{\text{III}}\text{-OOH}$  complex in the sulfoxidation reaction (Figure S11).

**DFT calculations.** A deeper understanding of the reaction itself was obtained using DFT calculations. As a starting point to model **1**, we used the published X-ray structure of  $[(\text{TMC})\text{Fe}^{\text{III}}(\text{O}_2)]^+$ , wherein the TMC methyl substituents are *cis* to  $\text{Fe-OO}$ .<sup>10a</sup> Figure 3 shows the energetics of the sulfoxidation

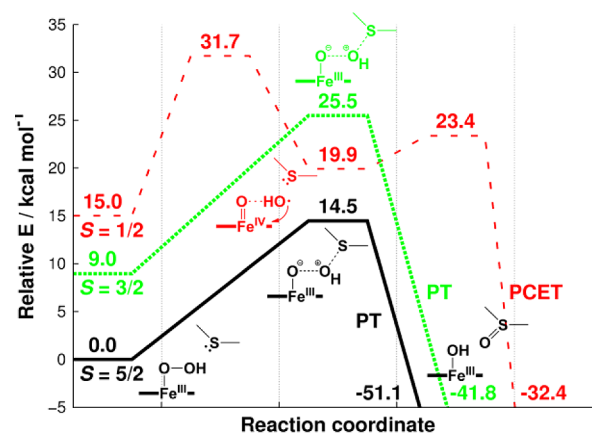


**Figure 3.** Calculated energy profiles for the sulfoxidation of thioanisole by **1**. While the  $S = 1/2$  state reacts via a stepwise, homolytic mechanism, the  $S = 3/2$  and  $5/2$  states react through a concerted heterolytic mechanism.

reaction of thioanisole by **1** at the B3LYP/LACVP\*\*//LACVP level<sup>18</sup> including the CPCM<sup>19</sup> solvation correction (trifluoroethanol) as implemented in Gaussian 09.<sup>20</sup> In agreement with experiments,<sup>10,11</sup> the  $S = 5/2$  HS state of **1** was found to be the ground state, with an Fe d-electron configuration of  $d_{xy}^1 d_{xz}^1 d_{yz}^1 d_{x^2-y^2}^2 d_z^1$ . The coordinate system was defined with the  $x$  axis along the O-OH bond and the  $z$  axis along the Fe-O bond, and orbital mixing with the peroxide moiety was disregarded for simplicity (see the DFT Section in the SI). The lowest-energy reaction proceeds through a concerted pathway in which O-O bond breaking occurs concomitantly with formation of the bond to the S atom of the substrate (Figure 1). The Mulliken spin density distribution (Table S5) showed that the leaving OH group has a spin of only 0.06 at the TS, indicating that the bond breaking is *heterolytic*. Further orbital analyses characterized the constituent groups at the TS as

$[\text{Fe}^{\text{III}}\text{O}]^+$  and  $\text{OH}^+$  (vide infra). This reaction is followed by a barrierless second step involving a return proton transfer (PT) from OH to form  $[(\text{TMC})\text{Fe}^{\text{III}}\text{OH}]^{2+}$ . The energy barrier for this reaction was found to be  $14.5 \text{ kcal mol}^{-1}$  (Figure 3); hence, the reaction is feasible from a theoretical point of view, in agreement with experiments. The  $S = 3/2$  intermediate-spin (IS) state ( $d_{xy}^2 d_{xz}^1 d_{yz}^1 d_{x^2-y^2}^1 d_z^0$ ) was found to follow the same reaction pathway but with a considerably higher TS ( $25.5 \text{ kcal mol}^{-1}$ ) and is therefore ruled out. Interestingly, computationally the reaction of the  $S = 1/2$  LS state ( $d_{xy}^2 d_{xz}^2 d_{yz}^1 d_{x^2-y^2}^0 d_z^0$ ) follows a stepwise pathway with a distinct intermediate. The spin density distribution on the leaving OH group corresponds to a half-radical at the intermediate stage, with another half-radical on the substrate S atom (Table S5). Together with orbital analyses, we interpret these data as showing a *homolytic* O–O bond cleavage that forms an  $[\text{Fe}^{\text{IV}}\text{O}]^{2+}$  compound with a loosely associated HO–S moiety sharing an unpaired electron. In the second step, the O–S bond is consolidated and a proton-coupled electron transfer (PCET) occurs, forming  $[(\text{TMC})\text{Fe}^{\text{III}}\text{OH}]^{2+}$ .

Even though the rate-limiting TS for the LS state lies too high to matter ( $31.7 \text{ kcal mol}^{-1}$ ), it still poses a fundamental question about the origins of this spin-state-dependent reactivity. Therefore, an in-depth analysis of the orbitals involved in the reaction was done in order to discern the factors that govern the choice of heterolytic versus homolytic O–O bond cleavage. Figure 4 describes the sulfoxidation reaction seen from an orbital-

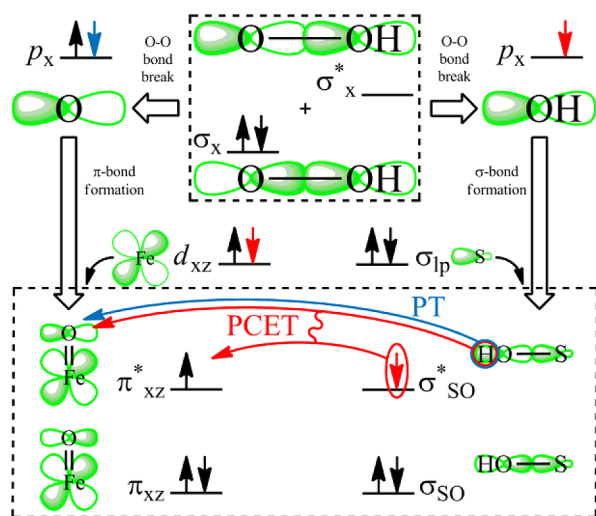


**Figure 4.** The most important orbitals involved in sulfoxidation by  $\text{Fe}^{\text{III}}\text{OOH}$ . Blue and red arrows represent electrons present only in the HS and LS configurations, respectively (black arrows denote electrons present in both). The fate of the two electrons in the  $\sigma_x$  orbital is different in homolytic (LS) and heterolytic (HS) bond breaking. This is governed by the number of electrons in the Fe  $d_{xz}$  orbital, which forms  $\pi_{xz}$  and  $\pi_{xz}^*$  orbitals with the  $p_x$  orbital of the proximal O (see the text).

mixing point of view. We found that during O–O bond breaking, the most important orbitals on the hydroperoxide ligand are the doubly occupied  $\sigma_x$  bonding orbital and the unoccupied  $\sigma_x^*$  antibonding orbital (Figure 4, top center). During the O–O bond breaking, these two orbitals split into their constituent  $p_x$  orbitals localized on each oxygen. The leaving OH group then forms a bond with the substrate S atom (Figure 4, right), where the orbital mixing results in a  $\sigma_{\text{SO}}$  bonding orbital and an  $\sigma_{\text{SO}}^*$  antibonding orbital. On the other hand, the  $p_x$  orbital of the proximal O mixes with the  $d_{xz}$  orbital of the iron to form the  $\pi_{xz}$

bonding and  $\pi_{xz}^*$  antibonding orbitals (Figure 4, left). If  $d_{xz}$  is doubly occupied, as in the LS case, its two electrons plus the one coming from the peroxide  $\sigma_x$  orbital will create a three-electron  $\pi_{xz}/\pi_{xz}^*$  system, whereas the remaining electron from the peroxide  $\sigma_x$  orbital will follow the leaving OH group to populate the  $\sigma_{\text{SO}}^*$  orbital (i.e., homolytic O–O bond breaking). This electron will then follow the proton back to the  $[(\text{TMC})\text{Fe}^{\text{IV}}\text{O}]^{2+}$  moiety in the PCET step. On the other hand, if  $d_{xz}$  is originally singly occupied, as in the IS and HS cases, the electron deficiency in the  $\pi_{xz}/\pi_{xz}^*$  system will favor heterolytic O–O bond breaking, in which both electrons in the peroxide  $\sigma_x$  orbital stay with the proximal oxygen. The final step of the reaction is therefore a pure PT. Hence, we find that *the number of electrons in the  $d_{xz}$  orbital governs the choice of heterolytic versus homolytic O–O bond cleavage in sulfoxidation reactions*. Although the above description is a somewhat simplified view (see the DFT Section text in SI), it is sufficiently useful to describe the underlying principles governing the reactions in all of the calculations presented here, including different spin states and ligands (vide infra).

To assess the generality of the above description of the orbital interactions, we also calculated the pathway for the sulfoxidation reaction catalyzed by **3** (Figure S12 and Tables S3, S6, and S9). The ground state of **3** was found to be the  $S = 1/2$  LS state, again in accord with experiments.<sup>11,15</sup> The rate-limiting TS:s here are at  $20.3$ ,  $29.3$ , and  $19.6 \text{ kcal mol}^{-1}$  for the LS, IS ( $S = 3/2$ ), and HS ( $S = 5/2$ ) states, respectively. The LS and HS TS:s are on the verge of what is considered to be accessible for slow reactions, leading to the prediction of a slow to no reaction using this ligand, in agreement with our experimental results showing no reactivity of this compound under the reaction conditions. Still, the calculations showed the same homolytic/heterolytic path selection depending on the occupation of the  $d_{xz}$  orbital as described above. Interestingly, we find for the high-energy  $S = 3/2$  state an example of a *homolytic, concerted* reaction, indicating that the homolytic and heterolytic bond breakings are not always equivalent to stepwise and concerted mechanisms, respectively. The pathway selection rule is kept for a third tested ligand (TPA, tris(2-pyridylmethyl)amine) (see SI, Tables S4, S7, and S10).

The above results can be put in a further general context. In a recent theoretical work<sup>11</sup> using **1** and **3** for C–H activation reactions with xanthene, the former one (in the  $S = 5/2$  ground state) was found to break the O–O bond heterolytically, with the substrate showing a spin of 0.33 at the TS. This is strikingly similar to the present sulfoxidation reaction results. For **3** ( $S = 1/2$  ground state), the O–O bond breaking occurred homolytically. While no electrons were donated from the substrate in this case, this is not required for homolytic O–O bond breaking, and the result is still in accord with our pathway selection rule.

In conclusion, we have provided the first direct experimental evidence demonstrating that HS  $\text{Fe}^{\text{III}}\text{OOH}$  species can perform sulfoxidation reactions, whereas LS  $\text{Fe}^{\text{III}}\text{OOH}$  species are much less reactive in OAT reactions. In contrast, the heme  $\text{Fe}^{\text{III}}\text{OOH}$  species, e.g. of the Cpd 0 type, is nonreactive in both sulfoxidation and H-abstraction reactions,<sup>21</sup> and cannot be invoked as a second oxidant in P450 and other heme systems or their analogs.<sup>6</sup> This difference between nonheme and heme  $\text{Fe}^{\text{III}}\text{OOH}$  species is an intriguing issue that is left for a future treatment. Furthermore, we have suggested a homolytic/heterolytic pathway selection rule based on the occupancy of the  $d_{xz}$  orbital in the sulfoxidation reactions by non-heme  $\text{Fe}^{\text{III}}\text{OOH}$  species: the reaction will occur homolytically if the  $d_{xz}$  orbital is doubly occupied and heterolytically otherwise. This rule



applies to all of the non-heme cases investigated here, regardless of the ligand and spin state.

## ■ ASSOCIATED CONTENT

### ■ Supporting Information

Experimental and DFT details, Tables S1–S10, Figures S1–S12, and complete ref 20 (as ref S7). This material is available free of charge via the Internet at <http://pubs.acs.org>.

## ■ AUTHOR INFORMATION

### Corresponding Author

sason@yfaat.ch.huji.ac.il; wwnam@ewha.ac.kr

### Author Contributions

<sup>||</sup>These authors contributed equally.

### Notes

The authors declare no competing financial interest.

## ■ ACKNOWLEDGMENTS

W.N. acknowledges support of this work by the NRF of Korea through CRI and GRL (2010-00353). S.S. acknowledges support by the Israeli Science Foundation. J.C. acknowledges the R&D (13-BD-0403) and GRDC (2012K1A4A3053565) programs of the MEST of Korea.

## ■ REFERENCES

- (1) (a) Nam, W. *Acc. Chem. Res.* **2007**, *40*, 465. (b) van Eldik, R. *Chem. Rev.* **2005**, *105*, 1917.
- (2) (a) Solomon, E. I.; Brunold, T. C.; Davis, M. I.; Kemsley, J. N.; Lee, S. K.; Lehnert, N.; Neese, F.; Skulan, A. J.; Yang, Y. S.; Zhou, J. *Chem. Rev.* **2000**, *100*, 235. (b) Abu-Omar, M. M.; Loaiza, A.; Hontzeas, N. *Chem. Rev.* **2005**, *105*, 2227. (c) Krebs, C.; Fujimori, D. G.; Walsh, C. T.; Bollinger, J. M., Jr. *Acc. Chem. Res.* **2007**, *40*, 484. (d) Bruijninx, P. C. A.; van Koten, G.; Klein Gebbink, R. J. M. *Chem. Soc. Rev.* **2008**, *37*, 2716. (e) Shaik, S.; Cohen, S.; Wang, Y.; Chen, H.; Kumar, D.; Thiel, W. *Chem. Rev.* **2010**, *110*, 949. (f) Rittle, J.; Green, M. T. *Science* **2010**, *330*, 933.
- (3) (a) Nam, W. *Acc. Chem. Res.* **2007**, *40*, 522. (b) Gunay, A.; Theopold, K. H. *Chem. Rev.* **2010**, *110*, 1060. (c) Borovik, A. S. *Chem. Soc. Rev.* **2011**, *40*, 1870. (d) Hohenberger, J.; Ray, K.; Meyer, K. *Nat. Commun.* **2012**, *3*, 720. (e) Mayer, J. M. *Acc. Chem. Res.* **2011**, *44*, 36. (f) de Visser, S. P.; Rohde, J.-U.; Lee, Y.-M.; Cho, J.; Nam, W. *Coord. Chem. Rev.* **2013**, *257*, 381.
- (4) (a) Newcomb, M.; Toy, P. H. *Acc. Chem. Res.* **2000**, *33*, 449. (b) Nam, W.; Ryu, Y. O.; Song, W. J. *J. Biol. Inorg. Chem.* **2004**, *9*, 654.
- (5) Metal–oxidant adducts, such as  $M^{n+}-OCl$  and  $M^{n+}-OIPh$ , have shown reactivities in oxygenation reactions, including thioanisole sulfoxidation. See: (a) Wang, C.; Kurahashi, T.; Fujii, H. *Angew. Chem., Int. Ed.* **2012**, *51*, 7809. (b) Cong, Z.; Yanagisawa, S.; Kurahashi, T.; Ogura, T.; Nakashima, S.; Fujii, H. *J. Am. Chem. Soc.* **2012**, *134*, 20617. (c) Lennartson, A.; McKenzie, C. J. *Angew. Chem., Int. Ed.* **2012**, *51*, 6767.
- (6) (a) Volz, T. J.; Rock, D. A.; Jones, J. P. *J. Am. Chem. Soc.* **2002**, *124*, 9724. (b) Cryle, M. J.; De Voss, J. J. *Angew. Chem., Int. Ed.* **2006**, *45*, 8221. (c) Wang, S. H.; Mandimutsira, B. S.; Todd, R.; Ramdhanie, B.; Fox, J. P.; Goldberg, D. P. *J. Am. Chem. Soc.* **2004**, *126*, 18. (d) Kerber, W. D.; Ramdhanie, B.; Goldberg, D. P. *Angew. Chem., Int. Ed.* **2007**, *46*, 3718. (e) Zhou, X.; Chen, X.; Jin, Y.; Markó, I. E. *Chem.—Asian J.* **2012**, *7*, 2253.
- (7) (a) Liu, L. V.; Bell, C. B.; Wong, S. D.; Wilson, S. A.; Kwak, Y.; Chow, M. S.; Zhao, J.; Hodgson, K. O.; Hedman, B.; Solomon, E. I. *Proc. Natl. Acad. Sci. U.S.A.* **2010**, *107*, 22419. (b) Neibergall, M. B.; Stubna, A.; Mekmouche, Y.; Müinck, E.; Lipscomb, J. D. *Biochemistry* **2007**, *46*, 8004. (c) Wada, A.; Ogo, S.; Nagatomo, S.; Kitagawa, T.; Watanabe, Y.; Jitsukawa, K.; Masuda, H. *Inorg. Chem.* **2002**, *41*, 616.
- (8) (a) Park, M. J.; Lee, J.; Suh, Y.; Kim, J.; Nam, W. *J. Am. Chem. Soc.* **2006**, *128*, 2630. (b) Franke, A.; Fertinger, C.; van Eldik, R. *Chem.—Eur. J.* **2012**, *18*, 6935.
- (9) (a) Ogliaro, F.; de Visser, S. P.; Cohen, S.; Sharma, P. K.; Shaik, S. J. *Am. Chem. Soc.* **2002**, *124*, 2806. (b) Derat, E.; Kumar, D.; Hirao, H.; Shaik, S. J. *Am. Chem. Soc.* **2006**, *128*, 473. (c) Li, C.; Zhang, L.; Zhang, C.; Hirao, H.; Wu, W.; Shaik, S. *Angew. Chem., Int. Ed.* **2007**, *46*, 8168.
- (10) (a) Cho, J.; Jeon, S.; Wilson, S. A.; Liu, L. V.; Kang, E. A.; Braymer, J. J.; Lim, M. H.; Hedman, B.; Hodgson, K. O.; Valentine, J. S.; Solomon, E. I.; Nam, W. *Nature* **2011**, *478*, 502. (b) Li, F.; Meier, K. K.; Cranswick, M. A.; Chakrabarti, M.; Van Heuvelen, K. M.; Müinck, E.; Que, L., Jr. *J. Am. Chem. Soc.* **2011**, *133*, 7256.
- (11) Liu, L. V.; Hong, S.; Cho, J.; Nam, W.; Solomon, E. I. *J. Am. Chem. Soc.* **2013**, *135*, 3286.
- (12) Kohn, W.; Sham, L. J. *Phys. Rev.* **1965**, *140*, A1133.
- (13) (a) Goto, Y.; Matsui, T.; Ozaki, S.; Watanabe, Y.; Fukuzumi, S. *J. Am. Chem. Soc.* **1999**, *121*, 9497. (b) Arias, J.; Newlands, C. R.; Abu-Omar, M. M. *Inorg. Chem.* **2001**, *40*, 2185. (c) Taki, M.; Itoh, S.; Fukuzumi, S. *J. Am. Chem. Soc.* **2002**, *124*, 998. (d) McPherson, L. D.; Drees, M.; Khan, S. I.; Strassner, T.; Abu-Omar, M. M. *Inorg. Chem.* **2004**, *43*, 4036. (e) Kumar, A.; Goldberg, I.; Botoshansky, M.; Buchman, Y.; Gross, Z. *J. Am. Chem. Soc.* **2010**, *132*, 15233.
- (14) It has been shown previously and confirmed here that the Fe product of the sulfoxidation,  $[(TMC)Fe^{III}(OH)]^{2+}$ , is unstable under our reaction conditions (e.g., in the presence of small amounts of  $H^+$  and 4-MTA). See: Braymer, J. J.; O'Neill, K. P.; Rohde, J.-U.; Lim, M. H. *Angew. Chem., Int. Ed.* **2012**, *51*, 5376.
- (15) Hazell, A.; McKenzie, C. J.; Nielsen, L. P.; Schindler, S.; Weitzer, M. *J. Chem. Soc., Dalton Trans.* **2002**, 310.
- (16) Although **3** could be prepared in 3:1 acetone/ $CF_3CH_2OH$  using a large amount of  $H_2O_2$  (80 equiv), we used  $CH_3OH$  as the solvent to reduce the amount of  $H_2O_2$  needed (10 equiv). The reactivity of **3** in the sulfoxidation reaction was not affected by the change in the solvent.
- (17) Park, J.; Morimoto, Y.; Lee, Y.-M.; Nam, W.; Fukuzumi, S. *J. Am. Chem. Soc.* **2012**, *134*, 3903.
- (18) (a) Becke, A. D. *Phys. Rev. A* **1988**, *38*, 3098. (b) Becke, A. D. *J. Chem. Phys.* **1993**, *98*, 1372. (c) Becke, A. D. *J. Chem. Phys.* **1993**, *98*, 5648. (d) Lee, C.; Yang, W.; Parr, R. G. *Phys. Rev. B* **1988**, *37*, 785. (e) Hay, P. J.; Wadt, W. R. *J. Chem. Phys.* **1985**, *82*, 299. (f) Dyall, K. G. *Theor. Chem. Acc.* **2004**, *112*, 403.
- (19) (a) Barone, V.; Cossi, M. *J. Phys. Chem. A* **1998**, *102*, 1995. (b) Cossi, M.; Rega, N.; Scalmani, G.; Barone, V. *J. Comput. Chem.* **2003**, *24*, 669.
- (20) Frisch, M. J.; et al. *Gaussian 09*, revision B.01; Gaussian, Inc.: Wallingford, CT, 2009.
- (21) For the sluggish reactivity of heme ferric hydroperoxide species in P450, as well as of synthetic corrole complexes, see: Wang, B.; Li, C.; Cho, K.-B.; Nam, W.; Shaik, S. *J. Chem. Theor. Comput.* **2013**, DOI: 10.1021/ct400190f.